Extracellular polymeric substance production in high rate algal oxidation ponds

Taobat A. Jimoh and A. Keith Cowan

ABSTRACT

Integrated algal pond systems (IAPSs) combine anaerobic and aerobic bioprocesses to affect sewage treatment. The present work describes the isolation and partial characterisation of soluble extracellular polymeric substances (EPSs) associated with microalgal bacterial flocs (MaB-flocs) generated in high rate algal oxidation ponds (HRAOPs) of an IAPS treating domestic sewage. Productivity and change in MaB-flocs concentration, measured as mixed liquor suspended solids (MLSS) between morning ($MLSS_{AM}$) and evening ($MLSS_{PM}$) were monitored and the substructure of the MaB-flocs matrix examined by biochemical analysis and Fourier transform infrared spectroscopy (FT-IR). Results show that MaB-flocs from HRAOPs are assemblages of microorganisms produced as discrete aggregates as a result of microbial EPS production. Formation and accumulation of the EPS was stimulated by light. Analysis by FT-IR revealed characteristic carbohydrate enrichment of these polymeric substances. In contrast, FT-IR spectra of EPSs from dark-incubated MaB-flocs confirmed that these polymers contained increased aliphatic and aromatic functionalities relative to carbohydrates. These differences, it was concluded, were due to dark-induced transition from phototrophic to heterotrophic metabolism. The results negate microalgal cell death as a contributor to elevated chemical oxygen demand of IAPS treated water.

Key words | extracellular polymeric substances, integrated algal pond system, microalgal bacterial flocs, wastewater

Taobat A. Jimoh
A. Keith Cowan (corresponding author)
Institute for Environmental Biotechnology,
Rhodes University (EBRU),
P.O. Box 94,
Grahamstown 6140,
South Africa
E-mail: *a.cowan@ru.ac.za*

INTRODUCTION

Integrated algal pond systems (IAPSs) are an established wastewater treatment technology and exploit the mutualistic relationship between bacteria and algae (Oswald 1995; Green *et al.* 1995; Munoz & Guieysse 2006; Park *et al.* 2011; Mambo *et al.* 2014; Craggs *et al.* 2015). During wastewater treatment by microalgal-bacterial (MaB) consortia, biomass accumulates due to CO_2 assimilation concomitant with *in situ* O_2 production. Heterotrophic bacteria consume O_2 for the aerobic biodegradation of organic compounds to CO_2, which is then assimilated by the microalgae. The continuous exchange of O_2 and CO_2 between microalgae and bacteria facilitates formation of microalgal-bacterial flocs (MaB-flocs) (Gutzeit *et al.* 2005; Medina & Neis 2007; Su *et al.* 2011). MaB-flocs typically consist of a consortium of microalgae, cyanobacteria and bacteria and may include a number of rotifers, ciliates and precipitates (Van Den Hende *et al.* 2011). Paddlewheel driven high rate oxidation ponds maintain these MaB-flocs in suspension as biological aggregates, presumably as components of a biofilm. Even so, IAPS treated water is characterized by elevated COD/TSS which led to recommendations that additional treatment of the outflow from algal settler ponds (ASPs) is required to meet specific discharge standards (Craggs *et al.* 2012; Mambo *et al.* 2014).

Extracellular polymeric substances (EPSs) are high-molecular weight compounds secreted into the environment and are responsible for the functional and structural integrity of biofilms (Staudt *et al.* 2004). Furthermore, EPS are considered the fundamental component that determines the physicochemical properties of a biofilm. In aquatic systems, EPS accumulate in the water when cells lyse or following secretion of high molecular weight compounds by microorganisms and, with the addition of organic matter, form matrices that serve as flocculants for biofilm formation (Sheng *et al.* 2010; More *et al.* 2014). Recent studies have elaborated on the downstream uses of these

doi: 10.2166/wst.2017.438

MaB-flocs, which emphasizes the value of this resource (Czaczyk & Myszka 2007; Natrah *et al.* 2013; Essam *et al.* 2013; Wieczorek *et al.* 2015; Arcila & Buitrón 2016; Coppens *et al.* 2016; Van Den Hende *et al.* 2016). The influence of EPS in wastewater treatment includes biofilm formation, adherence of cells to surfaces, enhanced settleability, and protection against harm from toxic substances and dewatering (Sutherland 2001; Sheng *et al.* 2010; More *et al.* 2014). Both soluble and bound EPS occur in MaB-flocs-containing wastewater treatment systems. Soluble EPS are loosely attached to cells or dissolved while bound EPS are closely associated with cells. These two forms of EPS can apparently be separated by centrifugation with the bound EPS forming a pellet and the soluble EPS remaining in the supernatant (Sheng *et al.* 2010). Although the composition of EPS varies depending on culture medium, population dynamic, growth phase of the organisms, and the extraction method adopted, the matrix of compounds in wastewater typically includes carbohydrates (in particular polysaccharides), proteins, humic substances, lipids, and uronic and nucleic acids (Wang *et al.* 2014). Consequently, these materials are of biotechnological importance and potential application in bioremediation, and the food and pharmaceutical industries, has been documented (Mishra & Jha 2009).

Previously, it was shown that effluent from the Belmont Valley IAPS had elevated levels of total suspended solids (TSS) and chemical oxygen demand (COD), which was considered to be the result of microalgal programmed cell death (Mambo *et al.* 2014). The present study describes the MaB-flocs formed in the high rate algal oxidation ponds (HRAOPs) of this IAPS and shows that loss of biomass is due to passive settling. Settleability and high effluent COD are attributed to formation of a soluble EPS associated with MaB-flocs generated in HRAOP of this IAPS.

MATERIALS AND METHODS

IAPS configuration and operation

The IAPS used in this study is located at the Belmont Valley Municipal WWTW, Grahamstown, South Africa (33° 19′ 07″ South, 26° 33′ 25″ East) and has a 75 $m^3\,d^{-1}$ design capacity equivalent to 500 persons. The system is in continuous operation and comprises of an in-pond digester (IPD), advanced facultative pond (AFP), two HRAOPs, and two ASPs configured in series. The typical process flow is: 3 d in the IPD → 20 d AFP → 2 d HRAOP A → 0.5 d ASP A → 4 d HRAOP B → 0.5 d ASP A → return to Belmont Valley WWTW inlet works. Although details on system configuration, process flow, and water treatment efficiency have been previously reported (Mambo *et al.* 2014) a flow diagram of the functioning of this IAPS is presented in Figure 1.

Productivity of MaB-flocs and preparation of EPS

Yield of MaB-flocs in HRAOP B was estimated by measuring mixed liquor suspended solids (MLSS) and by determining overall productivity as described by Banat *et al.* (1990). To achieve this, samples of mixed liquor were sourced directly from the front of the paddlewheel and transferred to the laboratory immediately. Both morning (09:00) and evening (16:30) samples were collected from August to November 2015 for seven consecutive 4 or 5 d periods. Thoroughly stirred samples were filtered under vacuum using pre-dried (105 °C × 1 h) glass fibre discs (Whatman; 47 mm, 0.45 μm) that had been placed in a desiccator for at least 30 min prior to use. After filtration of the final rinse (~3 min), discs were removed and dried

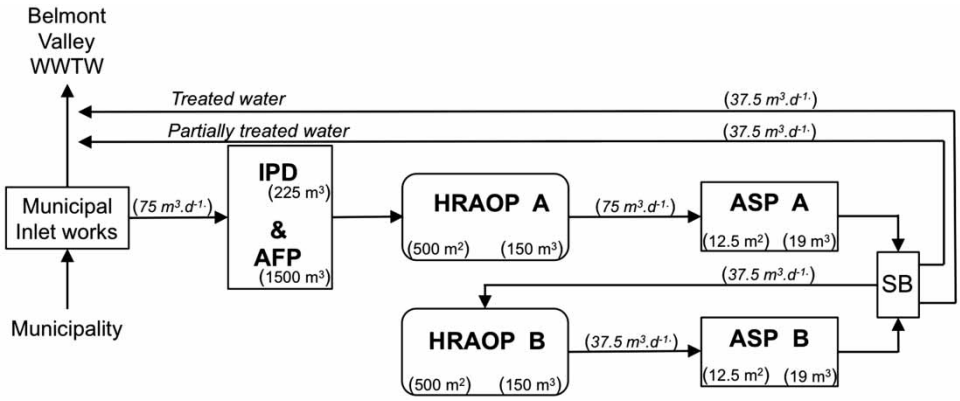

Figure 1 | Process flow and configuration of the experimental IAPS located at the Belmont Valley WWTW. Pond and reactor surface area, volume and flow rates are shown in parentheses. Effluent enters at the bottom of the IPD some 6 m below water level. SB = splitter box.

to a constant weight at 105 °C (1 h), cooled in a desiccator for 30 min, and the weight recorded. MLSS was calculated using the formula: MLSS (mg L^{-1}) = [(A – B) ×1,000] ÷ [Volume of sample in mL]. Where: A is the sample + filter weight; and B the weight of the filter only.

Pond productivity (g m^{-2} d^{-1}) was calculated by including the function C_s, which is the algal biomass in mg L^{-1}, determined by multiplying the MLSS (or TSS; APHA 1998) by a factor, n (i.e. the algal ratio in the TSS). Thus, HRAOP productivity was quantified per unit surface using the expression: $P = 10^{d}/_{t} \cdot n \cdot MLSS$. Where: P = MaB-flocs productivity (g m^{-2} d^{-1}); d = pond depth (m); t = detention time (d); SS= TSS (mg); and n = factor expressing the algal ratio in the suspended solids which, for near pure cultures is 0.9–1.0 (Al-Shayji *et al.* 1994).

Aliquots of wastewater (500 mL) were taken from HRAOP B and contained a mixed liquor comprising algae, diatoms, bacteria and other unidentified microorganisms. Flasks were placed in a controlled environment on a rotary shaker either under cool white fluorescent light or in total darkness at 25 °C. Aliquots were removed immediately (t = 0) and at 2, 3, 4, 6, 8, and 9 d intervals for quantification of EPS and biochemical analyses.

Only EPS released into the medium (i.e. soluble EPS) was extracted and, quantified by gravimetric analysis. Extraction was according to the method described by Ahmed *et al.* (2014). In brief, samples (100 mL) were centrifuged at 5,000 × g for 20 min, the supernatant was collected, MLSS removed by filtration (0.45 μm), and the aqueous filtrate filtered (0.22 μm), flash frozen using liquid nitrogen, freeze dried at −80 °C, weighed, and stored in a desiccator for further analysis.

Fourier transform infrared spectroscopy (FT-IR) analysis

FT-IR analysis of sub-samples of the extracted EPS (~1 mg) was carried out using a PerkinElmer Spectrum 100 instrument (PerkinElmer, Waltham, MA, USA) with attenuated total reflectance (ATR) accessory eliminating the need for mixing of samples with potassium bromide (KBr). The ATR accessory, fitted with a diamond top-plate, has spectral range of 25,000–100 cm^{-1}, refractive index of 2.4, and 2.01 μ depth of penetration. FT-IR spectra were recorded in the range of 4,000–650 cm^{-1}.

Biochemical analyses

Total carbohydrate, total protein, and total α-amino nitrogen of the extracted EPS were determined spectrophotometrically using the phenol sulphuric acid (Dubios *et al.* 1956), protein dye-binding (Bradford 1976), and Ninhydrin (Lie 1973) methods, respectively. For total carbohydrate, 2 mg aliquots of extracted EPS were resuspended in 0.5 mL distilled water to which was added, 0.5 mL of phenol solution (4% phenol in distilled water) followed immediately by 2.5 mL concentrated sulphuric acid (reagent grade). The mixture was vortexed and cooled to room temperature. Absorbance at 490 nm was determined using a UV-Vis spectrophotometer with distilled water and reagents used as background. Carbohydrate concentration was determined by interpolation from a standard curve for D-glucose (Dubios *et al.* 1956).

For total protein, 3 mg aliquots of extracted EPS were reconstituted in 0.5 mL of distilled water and 5 mL Bradford reagent (prepared by dissolving 100 mg of Coomassie Brilliant blue in 50 mL 95% ethanol and after addition of 100 mL 85% phosphoric acid, the solution was diluted to 1 L and filtered) added and, mixed thoroughly (Bradford 1976). Absorbance was measured at 595 nm after incubation for 10 min at room temperature and protein concentration determined by interpolation from a standard curve for bovine serum albumin.

For estimation of free α-amino nitrogen, 2 mg aliquots of EPS were dissolved in 2 mL distilled water and 1 mL of reagent (prepared by dissolving 100 g $Na_2HPO_4.12H_2O$, 60 g anhydrous KH_2PO_4, 5 g Ninhydrin, and 3 g fructose in 1 L distilled water, pH 6.7) added and placed in boiling water for 16 min and thereafter cooled to 20 °C (20 min). Dilution reagent (5 mL; prepared by dissolving 2 g KIO_3 in 600 mL distilled water which was then made to 1 L with 96% ethanol) was then added, samples thoroughly mixed, and absorbance at 570 nm determined spectrophotometrically within 30 min (Lie 1973). The concentration of α-amino nitrogen was determined by interpolation from a standard curve for glycine.

RESULTS

An example of the settleability and composition of the MaB-flocs produced in the HRAOPs of the pilot-scale IAPS treating municipal sewage during the course of this study are shown in Figure 2.

MaB-flocs appear as discrete entities and the bulk of these flocs settle readily within 2 h (Figure 2(a) and 2(b)). Light microscope analysis of these MaB-flocs revealed recruitment of microalgae, diatoms, cyanobacteria, and bacteria presumably facilitated by production of EPSs

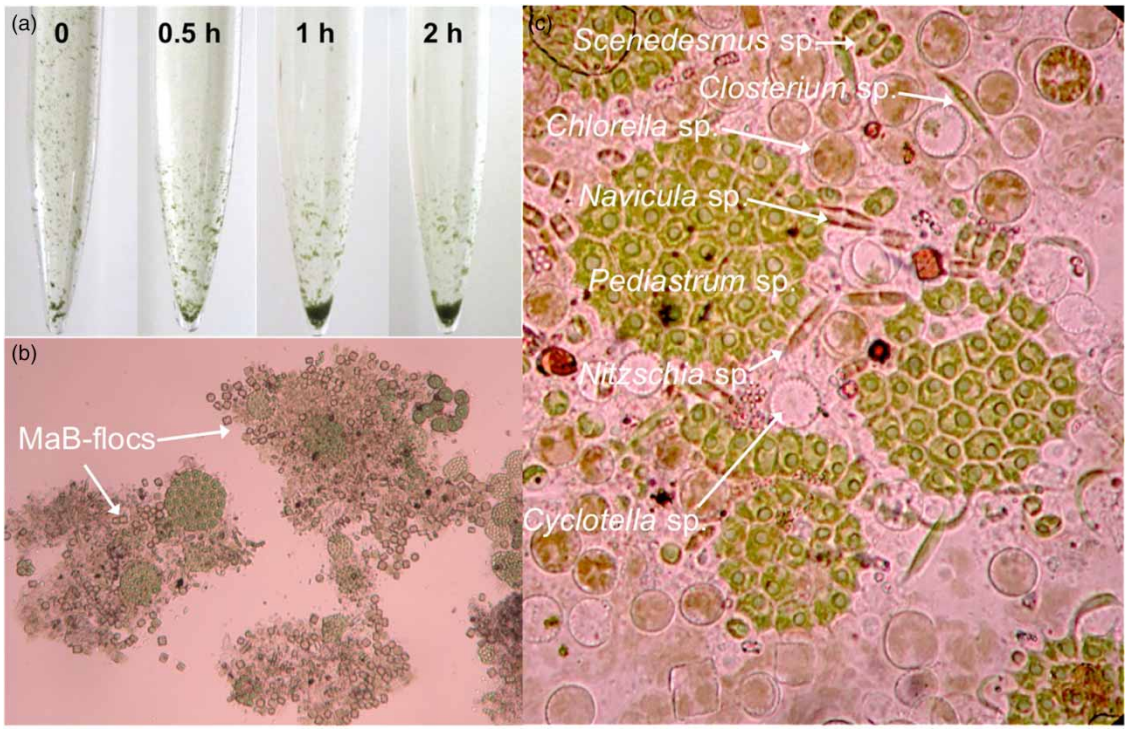

Figure 2 | Settleability and representative light microscope analysis of MaB-flocs generated in HRAOPs of an IAPS treating municipal sewage. (a) Settleability, (b) low resolution (10 ×), and (c) high resolution (40 ×) light microscope images of the MaB-flocs.

(Figure 2(c)). Among the more prominent species were the chlorophytes, *Pediastrum* sp., *Chlorella* sp., *Closterium* sp. and *Scenedesmus* sp. and the diatoms *Cyclotella* sp., *Nitzschia* sp. and *Navicula* sp.

In an effort to derive information about the formation of MaB-flocs two approaches were adopted. First, HRAOP productivity and the change in MaB-flocs concentration between morning ($MLSS_{AM}$) and evening ($MLSS_{PM}$) were monitored. Second, the substructure of the MaB-floc matrix was examined by a combination of biochemical analysis and FT-IR spectroscopy. As expected, production of MaB-flocs in HRAOPs, i.e. productivity measured as MLSS, gradually increased coincident with a rise in water temperature from ~10 g m^{-2} d^{-1} in early August (winter) to >20 g m^{-2} d^{-1} in November (Figure 3). This gradual increase in productivity with increasing water temperature was associated with a diurnal fluctuation in the accumulation of MLSS (Figure 3). As shown in Table 1, the loss of biomass between early evening, i.e. $MLSS_{PM}$ and the following morning ($MLSS_{AM}$) was due to continuous operation of the system and passive settling of the MaB-flocs in the ASP. Indeed, based on influent flow rate and hydraulic retention in the HRAOPs, the estimated loss of MLSS to the ASP between early evening and the following morning

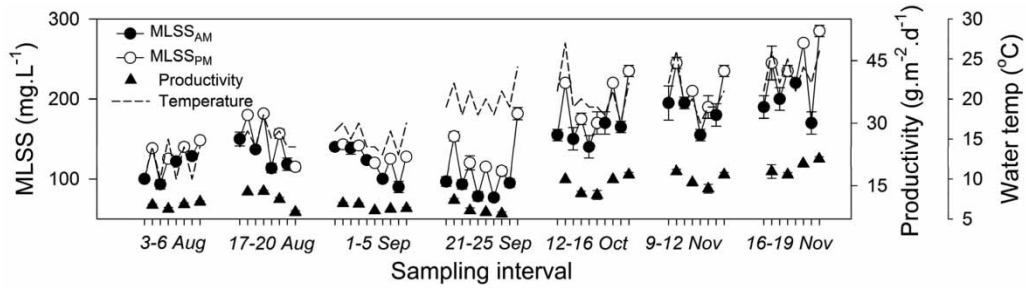

Figure 3 | Time course of the change in MaB-flocs productivity, and diurnal MLSS and water temperature in HRAOPs of an IAPS treating municipal sewage. Data were captured from August through November 2015 and are presented as the mean ± SE.

Table 1 | Diurnal fluctuation in MLSS concentration in the HRAOP of the IAPS treating municipal sewage

MLSS	mg L^{-1}
$MLSS_{PM}$	172.08 ± 9.52
$MLSS_{AM}$	135.48 ± 7.86
Measured loss of MLSS to ASP	36.70 ± 4.95 a
Estimated loss of MLSS to ASP	29.57 ± 1.60 a

$MLSS_{PM}$ and $MLSS_{AM}$ concentrations are mean values ± SE for all sampling intervals (Figure 3). Loss of MLSS was quantified as the difference between consecutive $MLSS_{PM}$ and $MLSS_{AM}$ determinations (i.e. $MLSS_{PM}$ – $MLSS_{AM}$) and is a mean value ± SE for all sampling intervals. Values followed by different letters are significantly different ($p \leq 0.001$). Estimated loss of MLSS between evening and the following morning was calculated using the expression $[(MLSS_{PM} \cdot V_P) - (\Delta t/24 \cdot V_D) \cdot MLSS_{PM}]/V_P$ where: V_P = pond volume (L); Δt = time difference (h); V_D = volume displaced (L); and, is a mean value ± SE for all sampling intervals. ASP = algal settler pond.

was 29.57 ± 1.60 mg L^{-1} which, using a *t* test (SigmaPlot Ver. 11; Systat Software, Inc., San Jose, CA, USA), was not significantly different ($P = 0.14$) from the measured loss of 36.70 ± 4.95 mg L^{-1}.

To gain further insight into the possible role for EPS in formation of MaB-flocs, the carbohydrate, protein and α-amino nitrogen contents were determined. In addition, the EPS from HRAOPs, and from MaB-flocs incubated in continuous light and total darkness were analysed by FT-IR spectroscopy. Results from two independent experiments revealed that the soluble EPS obtained after freeze-drying appeared as a white wispy-like material and that its production by MaB-flocs from HRAOPs was indeed enhanced by exposure to continuous illumination (Figure 4). Thus, soluble EPS increased from ~100 to >450 mg L^{-1} and from ~100 to ≥200 mg L^{-1} in light- and dark-incubated MaB-flocs, respectively.

The increase in recovery of soluble EPS over time was taken to indicate that production of EPS occurred concomitant with an increase in MLSS (Figure S1, Supplementary data, available with the online version of this paper). Even so, accumulation of this 'new' EPS by both light- and dark-incubated MaB-flocs was associated with a decline in carbohydrate, protein, and α-amino nitrogen content of the original material and, this decline was more pronounced for dark-incubated MaB-flocs (Figure 5(a) and 5(b)). Taken together, these results suggested that dark-incubated MaB-flocs transitioned from phototrophic to heterotrophic growth and that in the absence of light, both carbon and nitrogen were sourced mainly from already synthesized EPS. To elucidate this aspect further, the soluble EPS from HRAOPs and from MaB-flocs incubated in either continuous light or total darkness were extracted and analysed by FT-IR spectroscopy. Since the frequency at which a given vibration occurs is determined by the strength of the bonds involved and the mass of the component atoms, it was rationalised that EPS from dark-incubated MaB-flocs growing heterotrophically will differ in intensity of the characteristic functional groups from EPS formed in the light.

Comparative FT-IR spectra of the EPSs obtained after removal of MLSS from the HRAOP and from MaB-flocs incubated in either continuous light or total darkness are shown in Figure 6. A representative spectrum of EPS from HRAOP reveals characteristic functional groups (Figure 6(a)). The medium stretches and bend of frequency

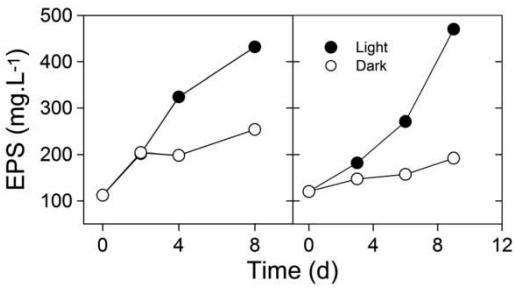

Figure 4 | Time course showing the accumulation of soluble EPS by MaB-flocs harvested from HRAOP of an IAPS treating municipal sewage incubated either in continuous light or total darkness. Data are from two independent experiments and are presented as the mean ± SE.

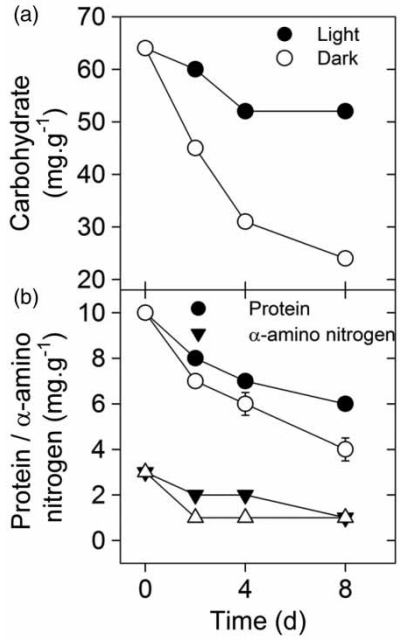

Figure 5 | Time course of the change in carbohydrate (a), protein and α-amino nitrogen (b) content of soluble EPS from MaB-flocs harvested from HRAOP of an IAPS treating municipal sewage incubated either in continuous light or total darkness. Data are representative of two independent experiments and are presented as the mean ± SE.

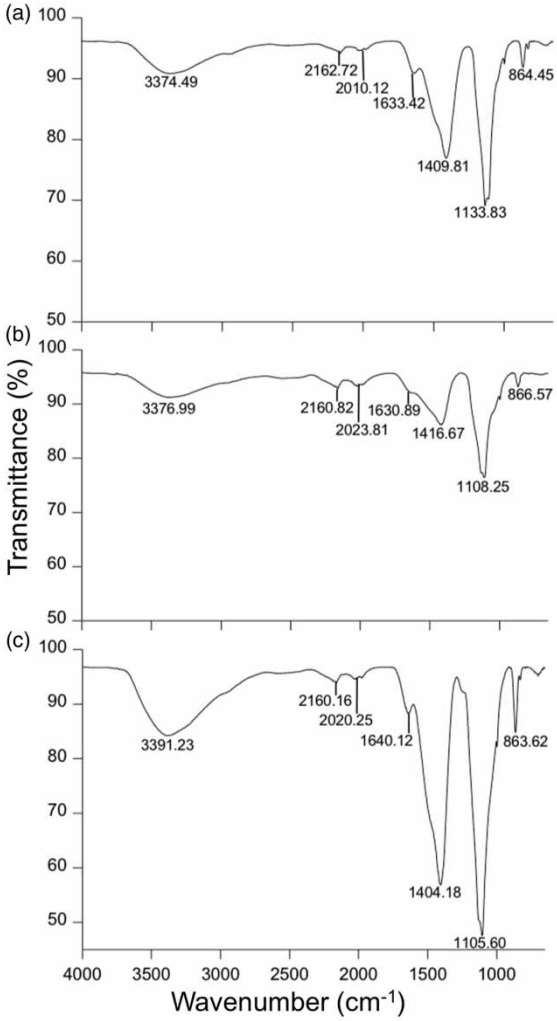

Figure 6 | Comparative FT-IR spectra of soluble EPSs extracted after removal of MLSS from the HRAOP (a) and from MaB-flocs incubated in either continuous light (b) or total darrkness (c).

in the spectral ranges 3,500–3,300 and 1,640–1,560 cm^{-1} were assigned to O-H (H-bonded) and N-H stretching. Weak absorbance at 2,940–2,920 cm^{-1} is attributed to assymetric C-H stretching of aliphatic methyl groups. The region 2,250–2,100 cm^{-1} is assigned to C≡C stretching of alkynes while the stretch, albeit weak, in the region of 1,660–1,600 cm^{-1} is assigned to C = C in alkenes but may be due either to CO_2 adsorption (Nabiev *et al.* 1976) or asymmetric stretching of –N = C = O– (Panda & Sadafule 1996). The sharp bend between 1,460 and 1,380 cm^{-1} is assigned to C-C of aromatics and, the region 1,300–1,000 cm^{-1} is assigned to stretching of C-O-C, C-O and corresponds to the presence of carbohydrates (Bremer & Geesey 1991; Bramhachari & Dubey 2006; Mishra & Jha 2009). The bending pattern in the region 950–650 cm^{-1} is assigned to sp^2 C-H of alkenes and aromatics. Taken together, the results of FT-IR analysis of EPS from HRAOPs confirmed the presence of primary amines, aromatic compounds, aliphatic alkyl groups, and carbohydrates. Similar spectra were derived from FT-IR analysis of EPSs from light-incubated MaB-flocs (Figure 6(b)). However, the IR spectrum of EPS from dark-incubated MaB-flocs revealed a substantial increase in intensity of absorbance in the vibrational ranges 3,500–2,800, 1,460–1,380, 1,300–1,000, and 950–650 cm^{-1} corresponding in assignment to O-H (H-bonded), N-H and sp C-H stretching, C-C bending of aliphatics and aromatics, O-C stretching and C-O-O bending of carbohydrates, and C-H bending and ring puckering of aromatics, respectively (Figure 6(c)). Thus, EPSs from dark-incubated MaB-flocs show increased frequency of vibration in aliphatic and aromatic functionalities relative to carbohydrates, presumably as a consequence of the transition to heterotrophic metabolism.

DISCUSSION

This study set out to determine the source of elevated TSS and COD in water from an IAPS treating domestic sewage. It was previously suggested that microalgal programmed cell death in both HRAOPs and ASPs might be responsible (Mambo *et al.* 2014). As shown in the present study, MaB-flocs are assemblages of microorganisms produced in HRAOPs as discreet aggregates and form as a result of microbial EPS production (Sheng *et al.* 2010; More *et al.* 2014). Formation of MaB-flocs in the HRAOPs increased with increasing water temperature and the transition from winter to summer. Inherent diurnal fluctuation in the concentration of MaB-flocs (measured as MLSS) and to a lesser extent EPS, in HRAOPs was due largely to passive removal of the flocs by the ASPs. Furthermore, formation and accumulation of loosely bound or soluble EPS was stimulated by light suggesting a link between photosynthesis and EPS production. Indeed, while EPS accumulation was observed in dark-incubated MaB-flocs the carbohydrate and protein content of these was markedly reduced relative to EPSs produced in continuous light. It was rationalised that dark incubation of MaB-flocs resulted in a transition from phototrophic to heterotrophic metabolism and that in the absence of photosynthesis, carbon and nitrogen from existing EPS was being recycled to support growth. Taken together, these results suggest that MaB-floc-derived EPS and not microalgal programmed cell death, appears to be

the major contributor to elevated TSS and COD in IAPS treated water.

Analysis by FT-IR of EPSs isolated after removal of MLSS from the HRAOP and MaB-flocs incubated in continuous light revealed characteristic carbohydrate enrichment of these polymeric substances (Mishra & Jha 2009). In contrast, FT-IR spectra of EPSs from dark-incubated MaB-flocs appeared to confirm that these polymers contained increased aliphatic and aromatic functionalities relative to carbohydrates. One possibility for these differences is recruitment of humic and/or fulvic substances. As pointed out by More *et al.* (2014), humic substances are an integral component of EPSs and are adsorbed by the EPS matrix from the natural environment rather than synthesized and secreted by microorganisms. Humics occur naturally as complex ligands and are widely distributed in aquatic systems and, in particular, sewage water and sediments. Since EPSs can adsorb humic acids and do so by a combination of hydrophobic and cationic bridging (Esparza-Soto & Westerhoff 2003), it is proposed that in darkness (or in the absence of photosynthesis as might be expected in ASPs) EPS-adsorbed humics and/or fulvics facilitate access to polymeric substance carbohydrates by MaB-flocs to sustain growth and metabolism without affecting the floc matrix.

CONCLUSION

Microbial (i.e. MaB-floc) EPS production rather than microalgal programmed cell death appears to be the major contributing factor towards elevated levels of TSS/COD of water from IAPS treating domestic sewage. The EPS from HRAOPs have been isolated and partially characterized. The FT-IR-spectra confirmed the presence of primary amines, aromatic-compounds, aliphatic alkyl groups and polysaccharides, whereas EPSs from dark-incubated MaB-flocs showed increased vibration in aliphatic and aromatic functionalities relative to carbohydrates. These differences, it was interpreted, were due to dark-induced transition from phototrophic to heterotrophic metabolism. Studies are currently underway to elucidate fully the structure of HRAOP EPSs and to evaluate any potential commercial application of these polymers for use in agriculture and industry and, as natural microbial flocculants. Precisely how MaB-floc EPS formation and accumulation impact design and operation of IAPS systems is also under consideration.

ACKNOWLEDGEMENTS

We gratefully acknowledge financial support from the Water Research Commission (WRC) of South Africa through WRC Projects (No. 7055 and 7164) awarded to Prof A. Keith Cowan of Rhodes University. Ms Taobat Jimoh acknowledges receipt of a graduate bursary from EBRU. This work was partially supported by a grant from the National Research Foundation, South Africa (IFR1202220169) awarded to Professor A. K. Cowan.

REFERENCES

Ahmed, M., Moerdijk-Poortvliet, T. C. W., Wijnholds, A., Stal, L. J. & Hasnain, S. 2014 Isolation, characterization and localization of extracellular polymeric substances from the cyanobacterium *Arthrospira platensis* strain MMG-9. *Euro. J. Phycol.* **49** (2), 143–150.

Al-Shayji, Y. A., Puskas, K., Al-Daher, R. & Esen, I. I. 1994 Production and separation of algae in a high-rate ponds system. *Environ. Intl.* **20** (4), 541–550.

APHA 1998 *Standard Methods for the Examination of Water and Wastewater.* 20th edn. American Public Health Association, Washington, DC, USA.

Arcila, J. S. & Buitrón, G. 2016 Microalgae–bacteria aggregates: effect of the hydraulic retention time on the municipal wastewater treatment, biomass settleability and methane potential. *J. Chem. Technol. Biotechnol.* **91** (11), 2862–2870.

Banat, I. M., Puskas, K., Esen, I. I. & Al-Daher, R. 1990 Wastewater treatment and algal productivity in an integrated ponding system. *Biol. Wastes* **32**, 265–275.

Bradford, M. M. 1976 A rapid and sensitive method for the quantification of microgram quantities of protein utilizing the principle of protein-dye binding. *Anal. Biochem.* **72**, 248–254.

Bramhachari, P. V. & Dubey, S. K. 2006 Isolation and characterization of exopolysaccharide produced by *Vibrio harveyi* strain VB23. *Lett. Appl. Microbiol.* **43**, 571–577.

Bremer, P. J. & Geesey, G. G. 1991 An evaluation of biofilms development utilizing non-destructive attenuated total reflectance Fourier transform infrared spectroscopy. *Biofoul.* **3**, 89–100.

Coppens, J., Grunert, O., Van Den Hende, S., Vanhoutte, I., Boon, N., Haesaert, G. & De Gelder, L. 2016 The use of microalgae as a high-value organic slow-release fertilizer results in tomatoes with increased carotenoid and sugar levels. *J. Appl. Phycol.* **28** (4), 2367–2377.

Craggs, R., Sutherland, D. & Campbell, H. 2012 Hectare-scale demonstration of high rate algal ponds for enhanced wastewater treatment and biofuel production. *J. Appl. Phycol.* **24** (3), 329–337.

Craggs, R., Park, J., Sutherland, D. & Heubeck, S. 2015 Economic construction and operation of hectare-scale wastewater treatment enhanced pond systems. *J. Appl. Phycol.* **27**, 1913–1922.

Czaczyk, K. & Myszka, K. 2007 Biosynthesis of extracellular polymeric substances (EPS) and its role in microbial biofilm formation. *Polish J. Environ. Stud.* **16** (6), 799–806.

Dubois, M., Gilles, K. A., Hamilton, J. K., Rebers, P. A. & Smith, F. 1956 Colorimetric method for determination of sugars and related substances. *Anal. Chem.* **28**, 350–356.

Esparza-Soto, M. & Westerhoff, P. 2003 Biosorption of humic and fulvic acids to live activated sludge biomass. *Water Res.* **37**, 2301–2310.

Essam, T., El Rakaiby, M. & Hashe, A. 2013 Photosynthetic based algal-bacterial combined treatment of mixtures of organic pollutants and CO_2 mitigation in a continuous photobioreactor. *World J. Microbiol. Biotechnol.* **29**, 969–974.

Green, F. B., Lundquist, T. J. & Oswald, W. J. 1995 Energetics of advanced integrated wastewater pond systems. *Water Sci. Technol.* **31** (12), 9–20.

Gutzeit, G., Lorch, D., Weber, A., Engels, M. & Neis, U. 2005 Bioflocculent algalbacterial biomass improves low-cost wastewater treatment. *Water Sci. Technol.* **52**, 9–18.

Lie, S. 1973 The EBC-Ninhydrin method for determination of free alpha amino nitrogen. *J. Inst. Brew.* **79** (1), 37–41.

Mambo, P. M., Westensee, D. K., Render, D. S. & Cowan, A. K. 2014a Operation of an integrated algae pond system for the treatment of municipal sewage: a South African case study. *Water Sci. Technol.* **69** (12), 2554–2561.

Medina, M. & Neis, U. 2007 Symbiotic algal bacterial wastewater treatment: Effect of food to microorganism ratio and hydraulic retention time on the process performance. *Water Sci. Technol.* **55**, 165–171.

Mishra, A. & Jha, B. 2009 Isolation and characterization of extracellular polymeric substances from micro-algae *Dunaliella salina* under salt stress. *Biores. Technol.* **100**, 3382–3386.

More, T. T., Yadav, J. S. S., Yan, S., Tyagi, R. D. & Surampalli, R. Y. 2014 Extracellular polymeric substances of bacteria and their potential environmental applications. *J. Environ. Mngt.* **144**, 1–25.

Munoz, R. & Guieysse, B. 2006 Algal-bacterial processes for the treatment of hazardous contaminants: a review. *Water Resource* **40** (15), 2799–2815.

Nabiev, B. A., Lafer, L. I., Yakerson, V. I. & Rubinshtein, A. M. 1976 IR spectra of catalysts and adsorbed molecules. *Russ. Chem. Bull.* **25**, 1398–1402.

Natrah, F. M. I., Bossier, P., Sorgeloos, P., Yusoff, F. M. d. & Defoirdt, T. 2013 Significance of microalgal–bacterial interactions for aquaculture. *Rev. Aquacult.* **5**, 1–14.

Oswald, W. J. 1995 Ponds in the twenty-first century. *Water Sci. Technol.* **31** (12), 1–8.

Panda, S. P. & Sadafule, D. S. 1996 FTIR spectral evaluation of polyurethane adhesive bonds in Perspex canopies of aircraft. *Defence Sci. J.* **46**, 171–174.

Park, J. B. K., Craggs, R. J. & Shilton, A. N. 2011 Wastewater treatment high rate algal ponds for biofuel production. *Biores. Technol.* **102**, 35–42.

Sheng, G.-P., Yu, H.-Q. & Li, X.-Y. 2010 Extracellular polymeric substances (EPS) of microbial aggregates in biological wastewater treatment systems: a review. *Biotech. Adv.* **28**, 882–894.

Staudt, C., Horn, H., Hempel, D. C. & Neu, T. R. 2004 Volumetric measurements of bacterial cells and extracellular polymeric substance glycoconjugates in biofilms. *Biotechnol. Bioeng.* **88** (5), 585–592.

Su, Y., Mennerich, A. & Urban, B. 2011 Municipal wastewater treatment and biomass accumulation with a wastewater-born and settleable algal-bacterial culture. *Water Res.* **45**, 3351–3358.

Sutherland, I. W. 2001 Biofilm exopolysaccharides: a strong and sticky framework. *Microbiology-SGM* **147**, 3–9.

Van Den Hende, S., Vervaeren, H., Saveyn, H., Maes, G. & Boon, N. 2011 Microalgal bacterial floc properties are improved by a balanced inorganic/organic carbon ratio. *Biotechnol. Bioeng.* **108**, 549–558.

Van Den Hende, S., Claessens, L., De Muylder, E., Boon, N. & Vervaeren, H. 2016 Microalgal bacterial flocs originating from aquaculture wastewater treatment as diet ingredient for *Litopenaeus vannamei* (Boone). *Aquacult. Res.* **47**, 1075–1089.

Wang, M., Kuo-Dahab, W. C., Dolan, S. & Park, C. 2014 Kinetics of nutrient removal and expression of extracellular polymeric substances of the microalgae, *Chlorella* sp. and *Micractinium* sp., in wastewater treatment. *Biores. Technol.* **154**, 131–137.

Wieczorek, N., Kucuker, M. A. & Kuchta, K. 2015 Microalgae-bacteria flocs (MaB-Flocs) as a substrate for fermentative biogas production. *Biores. Technol.* **194**, 130–136.

First received 27 October 2016; accepted in revised form 17 July 2017. Available online 28 July 2017